ACS OMEGA

http://pubs.acs.org/journal/acsodf

Article

Thin Films of Lanthanide Stearates as Modifiers of the Q-Sense Device Sensor for Studying Insulin Adsorption

Olga Ladikan, Elena Silyavka, Andrei Mitrofanov, Anastasia Laptenkova, Vladimir Shilovskikh, Petr Kolonitckii, Nikita Ivanov, Andrey Remezov, Anna Fedorova, Vassily Khripun, Olga Pestova, Ekaterina P. Podolskaya, Nikolai G. Sukhodolov, and Artem A. Selyutin*

Cite This: *ACS Omega* 2022, 7, 24973−24981

Read Online

ACCESS | Metrics & More | Article Recommendations | Supporting Information

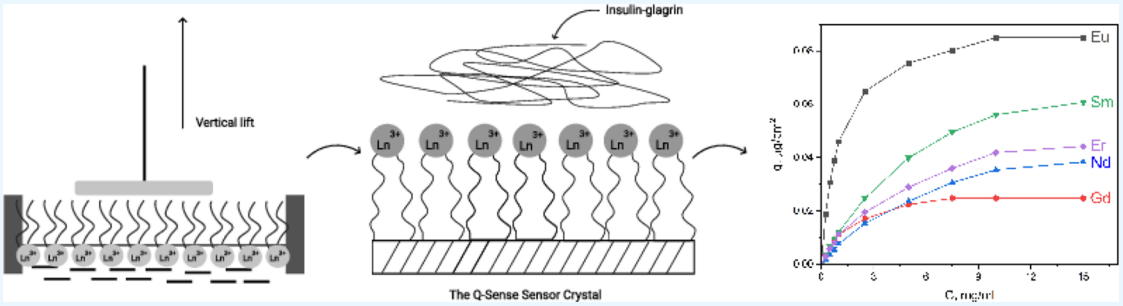

ABSTRACT: This article presents new possibilities of using thin films of lanthanide stearates as sorbent materials. Modification of the Q-sense device resonator with monolayers of lanthanide stearates by the Langmuir−Schaeffer method made it possible to study the process of insulin protein adsorption on the surface of new thin-film sorbents. The resulting films were also characterized by compression isotherms, chemical analysis, scanning electron microscopy, and mass spectrometry. The transition of stearic acid to salt was recorded by IR spectroscopy. Using the LDI MS method, the main component of thin films, lanthanide distearate, was established. The presence of Eu^{2+} in thin films was revealed. In the case of europium stearate, the maximum value of insulin adsorption was obtained, $-1.67 \cdot 10^{-10}$ mole/cm^2. The findings suggest the possibility of using thin films of lanthanide stearates as a sorption material for the proteomics determination of the quantitative protein content in complex fluid systems by specific adsorption on modified surfaces and isolation of such proteins from complex mixtures.

INTRODUCTION

The interest in the properties of thin films containing metal atoms,[1] such as Langmuir−Blodgett films (LBF), has not waned in recent years. Their initial studies were substantially related to salts of fatty acids and divalent metals.[2,3] The first studies of LBF began with cadmium stearate.[4] At the moment, the precipitation of cadmium stearates and other divalent metal stearates is the standard process for the preparation of LBF. Obtaining monolayers and LBF from trivalent metal ions and fatty acids was impossible for a long period of time.[4,5] The deposition of trivalent cation stearates poses a problem due to the impressive shear modulus of the monolayer on the surface of the subphase.[6] At the same time, ions of trivalent cations tend to hydrolysis and complexation more than divalent metals in an overwhelming number of cases; therefore, this problem is more relevant for trivalent ions. In this regard, works on these lanthanide salts were published much later, in spite of the fact that the production of such films was described in literature[7] and results of the preparation multilayer LBF from acids and trivalent metals were reported.[8,9] The techniques often used to obtain these structures are not standard and have only been studied for a small number of trivalent cations.[10−14] Despite the fact that yttrium is formally trivalent, the formation of films proceeded with ease, as with films containing ordinary divalent cations. Yttrium stearate was studied in ref 15, where it was shown that the ion fraction form of the yttrium content in the film depends on the pH of the subphase. During the study of yttrium arachidate films, it was found that the yttrium in the film is in the $Y(OH)^{2+}$ form.[16] However, it was observed that there is one Y^{3+} cation per three acid anions in LBF. This variety of compositional data of LBF has been obtained by different research groups using the same techniques.[14−17] This disparity can be explained by deviating the different conditions during the experiments. For lanthanum, the characteristics of monolayers were obtained due to stability,[18] contact angle,[19]

Received: December 27, 2021
Accepted: June 30, 2022
Published: July 14, 2022

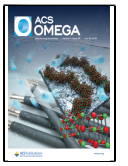

https://doi.org/10.1021/acsomega.1c07300
ACS Omega 2022, 7, 24973−24981

and shear viscosity[20] measurements. However, these measurements were most likely limited to a narrow range of application conditions. Although lanthanide salts of fatty acids have a wide range of applications, it is striking that there are so few fundamental works on the study of their physicochemical properties.[21] The superiority of lanthanide fatty acid salts over inorganic lanthanide salts lies in their solubility in molten polymers. Thus, it is possible to obtain transparent polymer fibers, films, and plates with trivalent lanthanide ions introduced into the composition.[22] The main advantages of optical polymer fibers in comparison with glass are low weight, low price, and ease of use.[23,24] Apropos, recent works have appeared in which monolayers containing ions of transition metals and lanthanides are used as sorption materials. In particular, these works investigate similar materials as adsorbents for bioorganic analysis.[25−34] Thin films transferred onto a substrate can act as metal-affinity sorbents. Such sorbents have an advantage because metals with an increased affinity for sites of biologically active macromolecules are accessible. This is due to the structure and method of transferring such films to the substrate. Researchers' interest remains in one of the object protein chemistry, namely, insulin. The use of this protein as a drug is still an extremely common procedure in improving the quality of life for patients with diabetes. The questions of searching for chromatographic methods for specific isolation and determination are still important.[35−41] Thin-film materials containing lanthanide atoms, as an example of nanotechnology, are actively used in many fields.[42−50] Also, materials containing lanthanide atoms are being actively studied as materials for bioorganic sensors,[51−53] including for determining the activity of insulin and analytical applications in the analysis of insulin content in complex systems.[1,54−56] Taking into account all of the problems associated with the production and application of such materials for proteomics, the purpose of this work is to demonstrate the possibility of using films containing lanthanide ions for insulin adsorption.

EXPERIMENTAL SECTION

Chemicals. The following reagents produced by Merck were used: lanthanum (7439-91-0), cerium (7440-45-1), praseodymium (7440-10-0), neodymium (7440-00-8), samarium (7440-19-9), europium (7440-53-1), gadolinium (7440-54-2), terbium (7440-27-9), dysprosium (7429-91-6), holmium (7440-60-0), erbium (7440-52-0), thulium (7440-30-4), ytterbium (7440-64-4), lutetium (7439-94-3), stearic acid (57-11-4, 95%), nitric acid (7697-37-2, 65−67%), hexane [110-54-3, puriss. p.a., ACS reagent, reag. Ph. Eur., ≥99% (GC)], and ammonia solution 25% (1336-21-6). All reagents were used without further purification, except stearic acid. For the purpose of recrystallization, a saturated solution of stearic acid in ethyl alcohol at 70 °C was prepared. Then this solution was cooled to 4 °C in a refrigerator. The crystals obtained were filtered under reduced pressure. The procedure mentioned above was repeated six times for each portion of the precipitated stearic acid crystals. Ultimately, colorless crystals of stearic acid were obtained, the yield of which was about 20%. These crystals were also measured for their melting point, which was 69.6 °C. Also, the purity of the obtained stearic acid was checked by FTIR and ^{1}H NMR spectroscopy. For the sorption process, insulin glargine produced by Sanofi-Aventis Deutschland GmbH company was used.

Obtaining Collapsed Lanthanide Stearate Films. For this, a weighed portion of recrystallized stearic acid equal to 0.0100 g was dissolved in 10 mL of hexane. Thus, a stearic acid solution with a concentration of 3.5×10^{-3} M was obtained. This concentration was chosen due to the ease of application and ease of control over the filling of the film on the surface. For the preparation of solutions of nitrates of lanthanides, the metal sample (3.0×10^{-4} mole) was dissolved in a minimum amount of nitric acid. Then the resulting solutions were diluted to a volume of 3 L to obtain solutions with a concentration 1.0×10^{-4} M. The pH of the aqueous subphase was eight. This value was fixed by adding nitric acid and ammonium hydroxide. To obtain films of lanthanide stearates, the Langmuir trough (self-made, size 600 mm × 250 mm × 20 mm) with movable barriers was filled with a solution of lanthanide nitrate, which was a subphase. A solution of stearic acid in hexane (250 μL) was applied to the surface of this solution. After the evaporation of hexane, the resulting film was compressed by movable barriers until collapse. The skimmed film was collected with a spatula.

Characterization. Many properties of collapsed thin films, such as a smooth surface accessible for interaction, a highly ordered structure, chemical composition, and thermal and mechanical strength, are identical to those of LB films. The possibility of using methods for studying collapsed monolayers as a way to study LB films was discovered.[57,58] Based on this, the resulting collapsed films were examined using scanning electron microscopy (SEM), element analysis, IR spectroscopy, mass spectrometry, and quantitative CHN analysis. To determine the parameters of the thin-film transfer to the sensor, the film compression isotherm and Brewster angle microscopy were recorded. The SEM study was carried out on a HITACHI S3400N electron microscope. In this work, the following parameters were used for shooting: exposure of 64 frames, an accelerating voltage of 20 kV, and a working distance of 10 mm (for secondary electrons). For element analysis in microscopy, an Oxford Instruments X-Max 20 Energy-Dispersive Spectrometer (EDX) attachment, which has an energy resolution of 127 eV for the Kα line for Mn, as well as an operating range from Be to Pu was used. The AzTec control software from Oxford Instruments was used to determine the elements by characteristic radiation, which was obtained due to the interaction of the electron beam with the sample substance and to obtain X-ray spectra. For the collection of electronic spectra, the following parameters were adopted: the acquisition time of one spectrum is 20 s; the probe current is 1.5 nA. For CHN analysis, a Euro EA3028-NT device was used, in which a dry sample with a mass of 1−10 mg was placed. For this purpose, 40 skimmed films of each stearate were placed in microtubes and dried in air. To carry out the mass spectrometric study, the target was preliminarily washed in an ultrasonic bath with water, alcohol, and hexane in turn. Then sample preparation was carried out. A total of 5−6 freshly prepared collapsed films of lanthanide stearates were transferred into microtubes and washed with water to get rid of the solutions of the corresponding lanthanide salts. After washing, water was removed from microtubes using a mechanical dispenser. Then, 0.5 mL of acetonitrile was added to each sample as a dispersing solvent. The samples were dispersed in an ultrasonic bath for 1−3 min. The obtained samples with dispersed films were applied to the target using a microdispenser without a matrix. Laser desorption/ionization mass spectrometry (LDI-MS) analysis

https://doi.org/10.1021/acsomega.1c07300
ACS Omega 2022, 7, 24973−24981

was performed on an Axima Perfomance MALDI-TOF-TOF time-of-flight mass spectrometer with a UV laser (337 nm). The range of detection of ions m/z was 100−1500 in positive mode. Mass spectra were processed using the MALDI-MS Shimadzu Biotech program. IR spectroscopy was carried out using a IRAffinity-1 spectrophotometer (Shimadzu, Japan) for operation in the UV, visible, and near-IR spectral range (from 4000 to 400 cm^{-1}). To obtain the spectra, we prepared a sample of collapsed lanthanide stearate films tablets with potassium bromide. The parameters of film transfer to the substrate were obtained in the course of studying film compression isotherms. Studying of surface pressure-area isotherms was carried out by continuous compression on the automatic installation consisting of a dural waxed bathtub (self-made, size 600 mm × 250 mm × 20 mm) in which studied solution was placed (subphase of lanthanide nitrates covered stearic acid in hexane). Langmuir's torsion scales with the sensitive sensor and a mobile barrier with the automatic mechanism of movement with a speed of 5 cm/min were connected to the system. Before the procedure for taking readings for compression isotherms, a calibration of the scales was made using weights. The formation and structuring process of insoluble stearic acid monolayers has been proven by Brewster angle microscopy using a BAM-1 instrument (NFT, Germany). The solution was placed in a Langmuir trough (length—20.5 cm, width—8 cm, bath area = 164 cm^2). Moving the barrier is possible in the range from 3 to 14 cm along the length of the tub, and images of the solution surface were taken at different film formation steps. To study sorption, a Q-sense E-4 (QSense Analyzer) (Biolin Scientific) device was used in the single-stream mode. The oscillation frequency of the crystal (quartz 5 MHz (QSX 303 SiO_2)) is related to the change in mass on the surface of the quartz resonator according to the Sauerbrey equation. The transfer of lanthanide stearate films was carried out by the Langmuir−Schaeffer method (horizontal lift) onto quartz resonators with deposited gold electrodes coated with SiO_2. For the transfer, the monolayer on the surface of the subphase in the Langmuir trough was brought into the state of a solid (close to collapse) two-dimensional object. The substrate touches this monolayer horizontally and peels it off, and the water droplets are dried with a stream of air. The control of the transfer of films to the substrate was carried out by measuring the shift of the basic characteristics of the detector, namely, the basic vibration frequency and basic energy loss. A modified quartz resonator was used to plot the adsorption isotherm of insulin glargine on the surface of a thin film of the stearate of the corresponding lanthanide. For this, insulin solutions with a given concentration (2.5, 5.0, 7.5, 10, 15, 20, 30, 40, 50, and 60 μg/mL) were sequentially passed through the measuring cell. The obtained curves were checked against the criterion of applicability of the Sauerbrey equation,[59] namely, by software methods; the increase in energy loss with an increase in the amount of adsorbed substance was estimated.

RESULTS AND DISCUSSION

The methods were utilized to establish the qualitative and quantitative composition of the resulted collapsed films. These properties and characteristics can be transferred to thin films of lanthanide stearates. It was they who modified the device's Q-sense sensor to determine the characteristics of the insulin adsorption process on lanthanide ions in films.

Infrared Spectroscopy. The transition of stearic acid to salt was confirmed by IR spectroscopy (Figure 1). The almost complete absence of a vibration band in the 1700 cm^{-1} region indicates the presence of only an ionized carboxyl group.

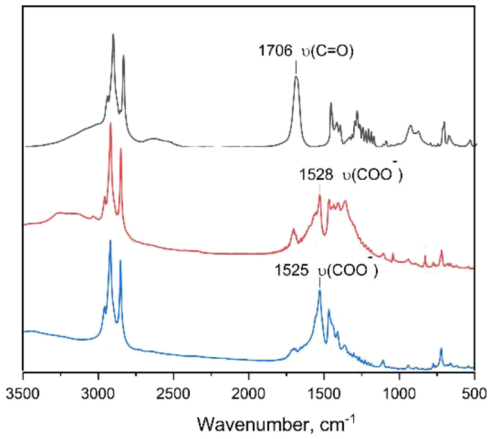

Figure 1. Infrared spectra of stearic acid (black) and stearates: Er (red), Ce (blue).

LDI-MS Analysis. After processing the obtained mass spectra and comparing them with the theoretically calculated isotope distribution, the presence of lanthanide stearate ions in the gas phase was determined. The given masses are presented in Table 1. The mass spectrometric analysis results confirmed the existence of the ion fraction form of lanthanide in monolayers. Experimental mass spectra revealed positively charged ions of lanthanide distearates, which are structural units of the studied films. This method was used to detect singly charged europium monostearate, which is a structural unit of the corresponding film. Such ions have also been found in films containing thulium and ytterbium. In europium, the bivalent state is very stable, which may be the reason for the absence of $EuSt^{2+}$ particles in the mass spectrum and the presence of special properties of such a film.

SEM with EDX Attachment. The presence of lanthanides in the films was also proved using the EDX method. Each sample contains only carbon atoms and the corresponding lanthanide. The presence of hydrogen atoms is not fixed by this method, and the number of oxygen atoms is too small for a qualitative determination. Spectra can be viewed in Figure S1. The study of the monolayer film morphology by SEM is hampered by instrumental capabilities. That is why it seems to us justified to consider the morphology of collapsed monolayers. The SEM results of collapsed lanthanide stearate monolayers are shown in Figure 2. In this series, the folding of the resulting structures is especially clearly observed. Since the compression of the monolayers occurred in two directions, zigzag folding is visible in the micrographs. Moreover, the formation of fragments with a smooth surface is visible. Microscopic studies using the SEM method show the presence of a folded structure of collapsed stearate-based monolayers, as well as smooth surface areas accessible for the sorption process. Thus, we can confirm the earlier assumptions about the similarity of the properties of strictly regular LB films, collapsed monolayers, and thin films of metal stearates.

CHN Analysis. Determining the quantitative content of lanthanide atoms in thin films or collapsed structures based on them is too complicated due to their extremely small amounts

https://doi.org/10.1021/acsomega.1c07300
ACS Omega 2022, 7, 24973−24981

Table 1. Monoizotopic Masses (m/z, Da) of the Ions Detected in the Mass Spectrum of Lanthanide Stearate Films

lanthanides	monostearate ($LnSt^+$)	distearate ($LnSt_2^+$)	tristearate ($LnSt_3H^+$)
La		705.43379	
Ce		706.43287	
Pr		707.43509	
Nd		708.43516	
Sm		718.44717	
Eu	436.18495		1003.72021
Gd		724.45154	
Tb		725.45278	
Dy		730.45661	
Ho		731.45776	
Er		732.45774	
Tm	452.19794	735.46166	
Yb	457.20258	740.46630	
Lu		741.46822	

in the composition. Thus, we decided to apply a different approach, previously described in the literature. Based on the data of a qualitative EDX analysis, which indicates the presence of lanthanide atoms in the composition of the corresponding films, we carried out a quantitative analysis for the content of the organic components of the films. To establish the molecular composition analysis of the films, the elemental composition of the samples was carried out. The analysis showed that when moving along the period, the mass fractions of carbon and hydrogen decrease, which is associated with an increase in the mass of the metal atom. Based on the experimental values (Table S1) of the mass content of carbon and hydrogen, according to the CHN analysis, the transfer ratios of stearic acid to the salt were calculated for each investigated lanthanide (Table 2). The transfer ratios were calculated based on three options for the composition of the materials obtained: $[(LnSt_3)_x(HSt)_{1-3x}]$ (1); $[(LnSt(OH)_2)_x(HSt)_{1-x}]$ (2); $[(LnSt_2OH)_x(HSt)_{1-2x}]$ (3) (Ln—lanthanides ions designation, St—stearate anion designation).

$$w(\mathrm{C}) = \frac{18M(\mathrm{C})}{(M(\mathrm{Ln}) + 3M(St))x + (M(\mathrm{HSt}))(1 - 3x)} \quad (1)$$

$$w(\mathrm{C}) = \frac{18M(\mathrm{C})}{(M(\mathrm{Ln}) + 2M(\mathrm{OH}) + M(St))x + (M(\mathrm{HSt}))(1 - x)} \quad (2)$$

$$w(\mathrm{C}) = \frac{18M(\mathrm{C})}{(M(\mathrm{Ln}) + M(\mathrm{OH}) + 2M(St))x + (M(\mathrm{HSt}))(1 - 2x)} \quad (3)$$

When calculating the fraction of the transition of stearic acid to the stearate of the corresponding lanthanide, it was noted that in the case of europium, a larger fraction of the transition is observed in comparison to other lanthanides. This may be due to the fact that, in addition to tristearate, europium can also form stable distearates.

Compression Isotherms. To determine the surface pressure values at which the solid thin-film transfer to the sensor surface will be carried out, studies of compression isotherms and an experiment on Brewster microscopy of the compression process were carried out. For stearic acid, the compression isotherm had two fairly obvious straight-line sections.[60−63] In the region of low values of surface pressure—less than 23 mN/m—it describes a two-dimensional liquid-stretched state. In the region of high values of surface pressure—more than 23 mN/m—it describes a two-dimensional crystalline state. The collapse pressure is 57 mN/m. By extrapolating the straight sections of the isotherm to zero surface pressure, the values of the area occupied by one molecule in these states were obtained. At low pressures, it was equal to 0.21 nm^2, and at high pressures, it was equal to 0.28 nm^2. $A_{2.5}$ is equal to 0.28 nm^2. The summary table (Table S2) shows the full parameters obtained due to compression isotherms for all lanthanide stearate films, and Figure 3 shows some general graphs of the experimental isotherms.

The compression isotherms' parameters (Table S1) indicated the similarity of the processes occurring during the compression and collapse of thin monomolecular films of stearic acid on the aqueous subphase containing lanthanide ions. The close radius of all lanthanide's ions and the same environment and coordination number are the reasons for the similarity of compression isotherms of lanthanide stearate films and their parameters. An increased value of the collapse pressure was noted in three cases: neodymium, samarium, and thulium. The values are higher than the surface tension values near water. The extreme values can be associated with the excellent temperature dependence of the surface tension of these stearates. Slight differences in the parameters of compression isotherms of stearates from stearic acid are clearly associated with the smaller ionic radius of lanthanides in comparison with the effective diameter of stearic acid. Based on these data, the parameters for transferring the obtained films of lanthanide stearates to the sensor were chosen. The pressure at which the transfer was carried out was 40−60 mN/m.

Brewster Angle Microscopy. Figure 4b shows an image of a monolayer taken immediately after its application to the water surface. When comparing this microphotograph with the microphotograph of the surface of a pure subphase, it can be seen that the monolayer remains on the surface of the subphase without going deep. This state of the monolayer can be attributed to the liquid-stretched state. Further, when the young layer is compressed by the mobile one, the monolayer is compacted (Figure 4c). With further displacement of the movable barrier, the monolayer was passed into a condensed state (Figure 4d); the surface has a pronounced solid character.

https://doi.org/10.1021/acsomega.1c07300
ACS Omega 2022, 7, 24973−24981

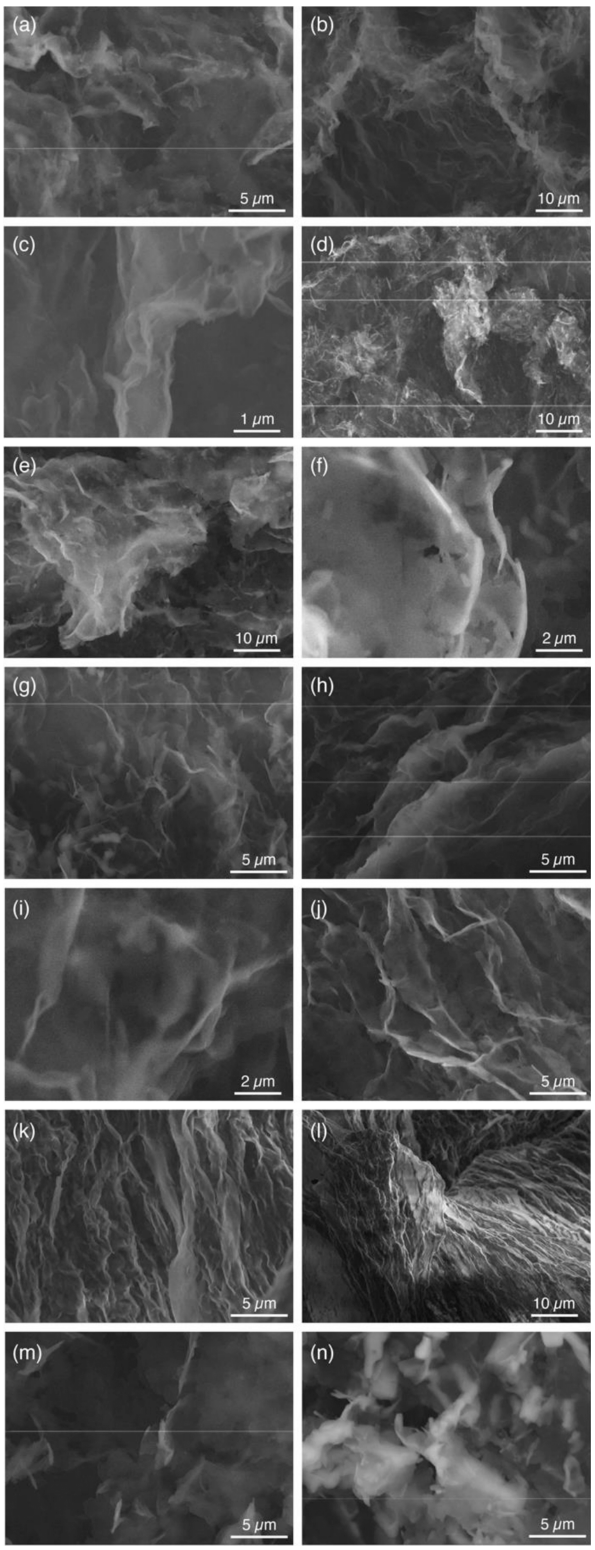

Figure 2. SEM micrographs of skimmed metal stearates LBF: (a) Ln, (b) Ce, (c) Pr, (d) Nd, (e) Sm, (f) Eu, (g) Gd, (h) Tb, (i) Dy, (j) Ho, (k) Er, (l) Tm, (m) Yb, and (n) Lu.

The values of the surface pressure at which the transition to the condensed state is observed agrees with the pressure obtained in the study of compression isotherms.

Transfer of monomolecular films onto a sensor was carried out by the Langmuir−Schaeffer method. For transfer, a solution of stearic acid in hexane was applied to the surface of the aqueous subphase with a salt of the corresponding lanthanide, and the resulting layer was pressed by barriers to a certain pressure. The pressure was determined from the values obtained from the compression isotherms (from 40 to 60 Nm/

Table 2. Transfer Ratios of Stearic Acid to the Salt, Calculated from the CHN Analysis

element	*x*		
	(1)	(2)	(3)
La	0.24	0.19	0.22
Ce	0.21	0.17	0.19
Pr	0.38	0.31	0.34
Nd	0.39	0.32	0.36
Sm	0.43	0.35	0.39
Eu	0.66	0.53	0.60
Gd	0.49	0.39	0.44
Tb	0.52	0.46	0.51
Dy	0.45	0.37	0.41
Ho	0.42	0.34	0.38
Er	0.53	0.43	0.48
Tm	0.49	0.40	0.44
Yb	0.55	0.44	0.49
Lu	0.48	0.39	0.42

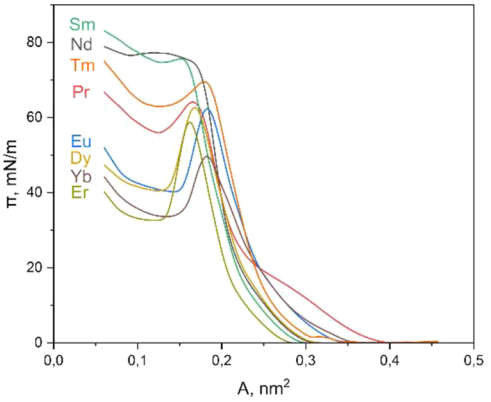

Figure 3. Compression isotherms of stearic acid on a subphase containing a salt solution: Sm (green), Nd (black), Tm (orange), Pr (red), Eu (blue), Dy (mustard), Yb (purple), and Er (olive).

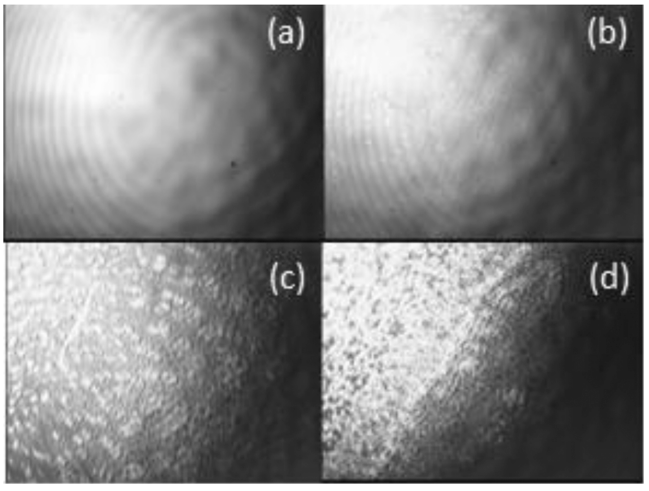

Figure 4. BAM images of the HSt layer (a) pure water; (b) first moment after addition of stearic acid dissolved in hexane; (c) at a surface compression; and (d) 3 min after surface formation.

https://doi.org/10.1021/acsomega.1c07300
ACS Omega 2022, 7, 24973−24981

m). Thus, solid films of lanthanide stearates oriented by hydrocarbon tails to the hydrophobized surface of the sensor were transferred to the sensor. The polar "heads", containing lanthanide atoms in their composition, were turned outward. This orientation of the monolayer made it possible to study the adsorption of the insulin protein on a surface consisting of lanthanide cations fixed on the surface of a thin solid film of stearates.

Insulin Glargine Sorption. The transfer of lanthanide stearate films was carried out by the Langmuir−Schaeffer method in such a way that the film uniformly covered the resonator surface and lanthanide atoms remained accessible for sorption. Prepared insulin glargine solutions with different insulin concentrations were passed through a cuvette with a stabilized film of one of the lanthanides on the resonator with increasing concentration. The solution was changed if the signal in a cell filled with a lower concentrated solution did not change for 2−4 min. The admissibility of such a change in concentrations was checked by a blank experiment in which this time period was determined experimentally. In Figure S1, one can see an example of analytical signal changes. After calculating the mass of adsorbed insulin, an isotherm of protein adsorption was built at a temperature of 25 °C. The calculation of adsorption was based on the area of the sensor, which was constant. Accordingly, the results of the specific adsorption per area were obtained. Figure 5 shows some general graphs of the experimental isotherms.

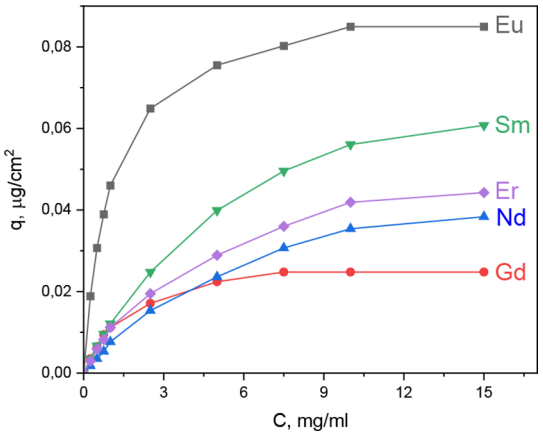

Figure 5. Insulin glargine sorption isotherms on thin film of europium stearate (black), samarium stearate (green), erbium stearate (purple), neodymium stearate (blue), and gadolinium stearate (red).

In ref 34, the influence of structural rearrangements of adsorbed proteins on the form of the adsorption isotherm was considered. The adsorption isotherm of type I and, consequently, a smooth kinetic curve (Figure 6a) corresponds to such adsorption, when at any orientation of the protein, completely reversible adsorption can be observed, while there is no protein−protein interaction.

The illustrations that correspond to b, c, and d show changes in the isotherm and kinetic curves of adsorption in the cases described below:

1. Protein molecules in one conformational or orientation form are reversibly adsorbed and then are able to pass into an irreversibly adsorbed state (Figure 6b);

2. Protein molecules with a transition from a reversibly adsorbed to an irreversibly adsorbed state change their conformation with an increase in the adsorption area. These initiate an increase in protein desorption (Figure 6c);

3. The adsorbed molecules rush to the irreversibly adsorbed state in full composition with a change in conformation (Figure 6d).

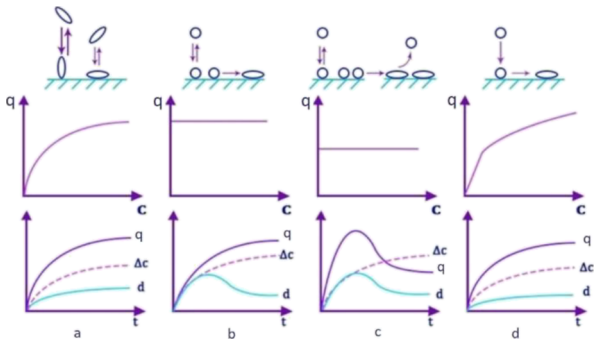

Figure 6. Types of protein−surface interaction and kinetic curves of adsorption and adsorption isotherms corresponding to them (d is the thickness of the protein layer, Δc is the amount of irreversibly adsorbed protein, and q is the amount of adsorbed protein.)

Let us consider the obtained isotherms of insulin adsorption on films. It should be noted that the protein is adsorbed without changing the configuration, according to Figure 6a. The plateau is a completely filled layer on the surface. It can be seen that the course of the curve for most of the presented isotherms is similar. For an accurate characterization, the adsorption isotherms were brought into a linearized form according to Langmuir ($1/\Gamma - 1/c$) and were also plotted in logarithmic coordinates ($\lg\Gamma - \lg c$). The constants of the Langmuir and Freundlich equations were found in the course of the study from the graphs. We can immediately conclude that the adsorption isotherms for neodymium and holmium stearates do not correspond to Freundlich's theory. Also, due to the fact that some lanthanides correspond to both equations, we used a comparison of the values of the reliability of the approximation. As a result, it was found that stearates of all lanthanides and lanthanum except europium are best described by Langmuir's theory (Table S3) and europium stearate by Freundlich's theory.

The maximum adsorption of insulin on films of lanthanide stearates correlates with the proportion of stearic acid to salt conversion in the films and not with the specific characteristics of lanthanides. A monotonic increase in the adsorption value of the plateau with the metal ion content in the film is observed. This fact indicates the metal-affinity mechanism of insulin adsorption on the surface of thin films. The adsorption of insulin protein on lanthanide stearate films is complex and cannot be unambiguously described by any single model. The correspondence of the obtained parameters of adsorption to the Freundlich model indicates the agglomeration and/or change in the structure of the protein during its adsorption on the film surface. This behavior can only be explained by the presence of a strong interaction of lanthanide ions with insulin sites. The findings suggest the possibility of using thin films of lanthanide stearates as a sorption material for the proteomics.

CONCLUSIONS

The application of a stearic acid solution in hexane to the aqueous subphase, which contains lanthanide salts, led to the formation of lanthanide stearates in the form of a thin film. As evidenced by the data of IR spectroscopy, stearic acid is almost

https://doi.org/10.1021/acsomega.1c07300
ACS Omega 2022, 7, 24973−24981

completely converted into a salt, which is accompanied by the disappearance of the vibration band of the non-ionized COOH group at about 1700 cm^{-1} from the spectrum. The CHN analysis results showed a very high proportion of the conversion of stearic acid to the corresponding lanthanide salt. LDI-MS spectra clearly proved that the structural link in the material obtained is lanthanide distearates. This situation was observed for all ions, except for europium. For films containing europium, the main link is monostearate. It can also be seen that for europium stearate films, the proportion of the stearic acid transition to the salt was higher. Compression isotherms of the structures obtained and their photomicrographs showed that it is possible to apply the structures obtained by the Langmuir−Schaeffer method onto a Q-sense quartz resonator. Such a modification of this device made it possible to study the process of the insulin protein adsorption on *f*-element ions in the lanthanide stearate thin solid films.

■ ASSOCIATED CONTENT

Supporting Information

The Supporting Information is available free of charge at https://pubs.acs.org/doi/10.1021/acsomega.1c07300.

Parameters of lanthanide stearate films compression isotherms, CHN analysis of lanthanide stearate films, and example of analytical signal changes at the Q-sense E-4 device (PDF)

■ AUTHOR INFORMATION

Corresponding Author

Artem A. Selyutin − *St. Petersburg State University, 199034 St. Petersburg, Russia;* orcid.org/0000-0002-5467-5658; Email: selutin@inbox.ru, a.selyutin@spbu.ru

Authors

Olga Ladikan − *St. Petersburg State University, 199034 St. Petersburg, Russia*

Elena Silyavka − *St. Petersburg State University, 199034 St. Petersburg, Russia*

Andrei Mitrofanov − *St. Petersburg State University, 199034 St. Petersburg, Russia; Leibniz-Institut für Polymerforschung Dresden e.V., 01069 Dresden, Germany;* orcid.org/0000-0002-4042-5164

Anastasia Laptenkova − *St. Petersburg State University, 199034 St. Petersburg, Russia*

Vladimir Shilovskikh − *St. Petersburg State University, 199034 St. Petersburg, Russia*

Petr Kolonitckii − *St. Petersburg State University, 199034 St. Petersburg, Russia*

Nikita Ivanov − *St. Petersburg State University, 199034 St. Petersburg, Russia*

Andrey Remezov − *St. Petersburg State University, 199034 St. Petersburg, Russia;* orcid.org/0000-0002-6173-4580

Anna Fedorova − *St. Petersburg State University, 199034 St. Petersburg, Russia*

Vassily Khripun − *St. Petersburg State University, 199034 St. Petersburg, Russia*

Olga Pestova − *St. Petersburg State University, 199034 St. Petersburg, Russia*

Ekaterina P. Podolskaya − *Golikov Research Center of Toxicology, 192019 St. Petersburg, Russia; Institute for Analytical Instrumentation of the Russian Academy of Science, 198095 St. Petersburg, Russia*

Nikolai G. Sukhodolov − *St. Petersburg State University, 199034 St. Petersburg, Russia; Institute for Analytical Instrumentation of the Russian Academy of Science, 198095 St. Petersburg, Russia*

Complete contact information is available at: https://pubs.acs.org/10.1021/acsomega.1c07300

Notes

The authors declare no competing financial interest.

■ ACKNOWLEDGMENTS

This research was funded by Russian Foundation for Basic Research (project No. 20-016-00160). The scientific research was performed at the Research park of St. Petersburg State University: Centre for Geo-Environmental Research and Modeling (GEOMODEL); Centre for Innovative Technologies of Composite Nanomaterials; Magnetic Resonance Research Centre; Chemical Analysis and Materials Research Centre; Centre for Optical and Laser Materials Research; Centre for Molecular and Cell Technologies; Centre for X-ray Diffraction Studies; Thermogravimetric and Calorimetric Research Centre; Centre for Physical Methods of Surface Investigation; Centre for Diagnostics of Functional Materials for Medicine, Pharmacology and Nanoelectronics; and Nanophotonics Centre.

■ REFERENCES

(1) Atkinson, P.; Murray, B. S.; Parker, D. A Cationic Lanthanide Complex Binds Selectively to Phosphorylated Tyrosine Sites, Aiding NMR Analysis of the Phosphorylated Insulin Receptor Peptide Fragment. *Org. Biomol. Chem.* **2006**, *4*, 3166.

(2) Gaines, G. L. *Insoluble Monolayers at Liquid-Gas Interfaces*; Interscience Publishers: New York, 1966; p 264.

(3) Binks, B. P. Insoluble Monolayers of Weakly Ionising Low Molar Mass Materials and Their Deposition to Form Langmuir-Blodgett Multilayers. *Adv. Colloid Interface Sci.* **1991**, *34*, 343−432.

(4) Blodgett, K. B. Films Built by Depositing Successive Monomolecular Layers on a Solid Surface. *J. Am. Chem. Soc.* **1935**, *57*, 1007−1022.

(5) Ando, Y.; Hiroike, T.; Miyashita, T.; Miyazaki, T. Magnetic Properties of Stearate Films with 3d Transition Metal Ions Fabricated by the Langmuir-Blodgett Method. *Thin Solid Films* **1996**, *278*, 144−149.

(6) Abraham, B. M.; Ketterson, J. B.; Miyano, K.; Kueny, A. Shear Rigidity of Spread Stearic Acid Monolayers on Water. *J. Chem. Phys.* **1981**, *75*, 3137−3141.

(7) Faridbod, F.; Ganjali, M. R.; Hosseini, M. Lanthanide Materials as Chemosensors. In *Lanthanide-Based Multifunctional Materials*; Elsevier, 2018; pp 411−454.

(8) Kitchen, J. A.; Barry, D. E.; Mercs, L.; Albrecht, M.; Peacock, R. D.; Gunnlaugsson, T. Circularly Polarized Lanthanide Luminescence from Langmuir-Blodgett Films Formed from Optically Active and Amphiphilic EuIII-Based Self-Assembly Complexes. *Angew. Chem., Int. Ed.* **2012**, *124*, 728−732.

(9) Lu, Q.; Luo, Y.; Li, L.; Liu, M. Self-Assembled Supramolecular Architecture of a Bolaamphiphilic Diacid on the Subphases Containing Ag(I) and Eu(III) Metal Ions. *Langmuir* **2003**, *19*, 285−291.

(10) Xie, F.; Zhuo, C.; Hu, C.; Liu, M. H. Evolution of Nanoflowers and Nanospheres of Zinc Bisporphyrinate Tweezers at the Air/Water Interface. *Langmuir* **2017**, *33*, 3694−3701.

(11) Galanti, A.; Kotova, O.; Blasco, S.; Johnson, C. J.; Peacock, R. D.; Mills, S.; Boland, J. J.; Albrecht, M.; Gunnlaugsson, T. Exploring the Effect of Ligand Structural Isomerism in Langmuir-Blodgett Films of Chiral Luminescent Eu III Self-Assemblies. *Chem. −A Eur. J.* **2016**, *22*, 9709−9723.

(12) Qu, N.; Sun, S.; Zhao, Q.; Jiao, T.; Zhou, J.; Xing, R.; Gao, F.; Zhang, L.; Peng, Q. Self-Assembled Composite Langmuir Films via Fluorine-Containing Bola-Type Derivative with Metal Ions. *Coatings* **2018**, *8*, 141.
(13) Bukreeva, T. V. Langmuir−Blodgett Films of Fatty Acid Salts of Bi- and Trivalent Metals: Y, Ba, and Cu Stearates. *Colloid J.* **2003**, *65*, 134−140.
(14) Fanucci, G. E.; Seip, C. T.; Petruska, M. A.; Nixon, C. M.; Ravaine, S.; Talham, D. R. Organic/Inorganic Langmuir−Blodgett Films Based on Known Layered Solids: Divalent and Trivalent Metal Phosphonates. *Thin Solid Films* **1998**, *327*−*329*, 331−335.
(15) Zotova, T.; Arslanov, V.; Gagina, I. Monolayers and Langmuir−Blodgett Films of Yttrium Stearate. *Thin Solid Films* **1998**, *326*, 223−226.
(16) Schurr, M.; Brandl, D.; Tomaschko, C.; Schoppmann, C.; Voit, H. Langmuir—Blodgett Films Made from Yttrium Arachidate. *Thin Solid Films* **1995**, *261*, 271−274.
(17) Johnson, D. J.; Amm, D. T. Comment on "Deposition of Yttrium Ions in Langmuir-Blodgett Films Using Arachidic Acid.". *Langmuir* **1994**, *10*, 1632−1632.
(18) Aveyard, R.; Binks, B. P.; Carr, N.; Cross, A. W. Stability of Insoluble Monolayers and Ionization of Langmuir-Blodgett Multilayers of Octadecanoic Acid. *Thin Solid Films* **1990**, *188*, 361−373.
(19) Buhaenko, M. R.; Richardson, R. M. Measurements of the Forces of Emersion and Immersion and Contact Angles during Langmuir-Blodgett Deposition. *Thin Solid Films* **1988**, *159*, 231−238.
(20) Buhaenko, M. R.; Goodwin, J. W.; Richardson, R. M. Surface Rheology of Spread Monolayers. *Thin Solid Films* **1988**, *159*, 171−189.
(21) Ivanin, S. N.; Buz'ko, V. Y.; Panyushkin, V. T. Research of the Properties of Gadolinium Stearate by EPR Spectroscopy. *Russ. J. Coord. Chem.* **2021**, *47*, 219−224.
(22) Liu, L.; Chen, M.; Yang, J.; Liu, S.-Z.; Du, Z.-L.; Wong, W.-Y. Preparation, Characterization, and Electrical Properties of Dual-Emissive Langmuir-Blodgett Films of Some Europium-Substituted Polyoxometalates and a Platinum Polyyne Polymer. *J. Polym. Sci., Part A: Polym. Chem.* **2010**, *48*, 879−888.
(23) Seyrek, E.; Decher, G. Layer-by-Layer Assembly of Multifunctional Hybrid Materials and Nanoscale Devices. In *Polymer Science: A Comprehensive Reference*; Elsevier, 2012; pp 159−185.
(24) Binnemans, K. Rare-Earth Beta-Diketonates. In *Handbook on the Physics and Chemistry of Rare Earths*; Elsevier: Amsterdam, 2005; pp 107−272.
(25) Bobrysheva, N. P.; Ivanov, N. S.; Selyutin, A. A.; Janklovich, A. I.; Sukhodolov, N. G. Magnetic Properties of Langmuir-Blodgett Films with Iron Ions. *Rev. Adv. Mater. Sci.* **2014**, *37*, 48−52.
(26) Gladilovich, V.; Greifenhagen, U.; Sukhodolov, N.; Selyutin, A.; Singer, D.; Thieme, D.; Majovsky, P.; Shirkin, A.; Hoehenwarter, W.; Bonitenko, E.; Podolskaya, E.; Frolov, A. Immobilized Metal Affinity Chromatography on Collapsed Langmuir-Blodgett Iron(III) Stearate Films and Iron(III) Oxide Nanoparticles for Bottom-up Phosphoproteomics. *J. Chromatogr. A* **2016**, *1443*, 181−190.
(27) Shreyner, E. V.; Alexandrova, M. L.; Sukhodolov, N. G.; Selyutin, A. A.; Podolskaya, E. P. Extraction of the Insecticide Dieldrin from Water and Biological Samples by Metal Affinity Chromatography. *Mendeleev Commun.* **2017**, *27*, 304−306.
(28) Podolskaya, E. P.; Serebryakova, M. V.; Krasnov, K. A.; Grachev, S. A.; Gzgzyan, A. M.; Sukhodolov, N. G. Application of Langmuir−Blodgett Technology for the Analysis of Saturated Fatty Acids Using the MALDI-TOF Mass Spectrometry. *Mendeleev Commun.* **2018**, *28*, 337−339.
(29) Podolskaya, E. P.; Gladchuk, A. S.; Keltsieva, O. A.; Dubakova, P. S.; Silyavka, E. S.; Lukasheva, E.; Zhukov, V.; Lapina, N.; Makhmadalieva, M. R.; Gzgzyan, A. M.; Sukhodolov, N. G.; Krasnov, K. A.; Selyutin, A. A.; Frolov, A. Thin Film Chemical Deposition Techniques as a Tool for Fingerprinting of Free Fatty Acids by Matrix-Assisted Laser Desorption/Ionization Time-of-Flight Mass Spectrometry. *Anal. Chem.* **2019**, *91*, 1636−1643.
(30) Silyavka, E. S.; Selyutin, A. A.; Sukhodolov, N. G.; Shilovskikh, V. V.; Oleneva, P. A.; Mitrofanov, A. A.; Keltsieva, O. A.; Dubakova, P. S.; Babakov, V. N.; Alexandrova, M. L.; Krasnov, N. V.; Podolskaya, E. P. Collapsed Monomolecular Thin Films as Surface Nanomodification Techniques for Bioorganic MALDI. *Analysis* **2019**, No. 030015.
(31) Babakov, V. N.; Shreiner, E. V.; Keltsieva, O. A.; Dubrovskii, Y. A.; Shilovskikh, V. V.; Zorin, I. M.; Sukhodolov, N. G.; Zenkevich, I. G.; Podolskaya, E. P.; Selyutin, A. A. Application of Lanthanum Stearate Monolayers as a Metal-Affinity Sorbent for the Selective Sorption of Soman Adducts to Human Serum Albumin. *Talanta* **2019**, *195*, 728−731.
(32) Gladchuk, A.; Shumilina, J.; Kusnetsova, A.; Bureiko, K.; Billig, S.; Tsarev, A.; Alexandrova, I.; Leonova, L.; Zhukov, V. A.; Tikhonovich, I. A.; Birkemeyer, C.; Podolskaya, E.; Frolov, A. High-Throughput Fingerprinting of Rhizobial Free Fatty Acids by Chemical Thin-Film Deposition and Matrix-Assisted Laser Desorption/Ionization Mass Spectrometry. *Methods Protoc.* **2020**, *3*, 36.
(33) Stepashkin, N. A.; Chernenko, M. K.; Khripun, V. D.; Ivanov, N. S.; Sukhodolov, N. G. Electrochemical Properties of Langmuir-Blodgett Films Containing Cobalt Hexacyanoferrate Nanoparticles. *Thin Solid Films* **2018**, *661*, 1−6.
(34) Ivanov, N. S.; Khripun, V. D.; Trofimov, M. A.; Sukhodolov, N. G.; Pendin, A. A. Synthesis of Nanodimensional Films Based on Hybrid Materials and Their Application in the Ion-Selective Electrodes. *Rev. Adv. Mater. Sci.* **2014**, *39*, 34−40.
(35) Fuchs, S.; Ernst, A. U.; Wang, L.-H.; Shariati, K.; Wang, X.; Liu, Q.; Ma, M. Hydrogels in Emerging Technologies for Type 1 Diabetes. *Chem. Rev.* **2021**, *121*, 11458−11526.
(36) Hühmer, A. F. R.; Aced, G. I.; Perkins, M. D.; Gürsoy, R. N.; Jois, D. S. S.; Larive, C.; Siahaan, T. J.; Schöneich, C. Separation and Analysis of Peptides and Proteins. *Anal. Chem.* **1997**, *69*, 29−58.
(37) Karas, J. A.; Wade, J. D.; Hossain, M. A. The Chemical Synthesis of Insulin: An Enduring Challenge. *Chem. Rev.* **2021**, *121*, 4531−4560.
(38) Larive, C. K.; Lunte, S. M.; Zhong, M.; Perkins, M. D.; Wilson, G. S.; Gokulrangan, G.; Williams, T.; Afroz, F.; Schöneich, C.; Derrick, T. S.; Middaugh, C. R.; Bogdanowich-Knipp, S. Separation and Analysis of Peptides and Proteins. *Anal. Chem.* **1999**, *71*, 389−423.
(39) D'Atri, V.; Fekete, S.; Clarke, A.; Veuthey, J.-L.; Guillarme, D. Recent Advances in Chromatography for Pharmaceutical Analysis. *Anal. Chem.* **2019**, *91*, 210−239.
(40) Zheng, J.; Chen, X.; Yang, Y.; Tan, C. S. H.; Tian, R. Mass Spectrometry-Based Protein Complex Profiling in Time and Space. *Anal. Chem.* **2021**, *93*, 598−619.
(41) Soffe, R.; Nock, V.; Chase, J. G. Towards Point-of-Care Insulin Detection. *ACS Sens.* **2019**, *4*, 3−19.
(42) Ullstad, F.; Bioletti, G.; Chan, J. R.; Proust, A.; Bodin, C.; Ruck, B. J.; Trodahl, J.; Natali, F. Breaking Molecular Nitrogen under Mild Conditions with an Atomically Clean Lanthanide Surface. *ACS Omega* **2019**, *4*, 5950−5954.
(43) Jiang, L.; Li, J.; Xia, D.; Gao, M.; Li, W.; Fu, D.-Y.; Zhao, S.; Li, G. Lanthanide Polyoxometalate Based Water-Jet Film with Reversible Luminescent Switching for Rewritable Security Printing. *ACS Appl. Mater. Interfaces* **2021**, *13*, 49462−49471.
(44) Kumi Barimah, E.; Rahayu, S.; Ziarko, M. W.; Bamiedakis, N.; White, I. H.; Penty, R. V.; Kale, G. M.; Jose, G. Erbium-Doped Nanoparticle−Polymer Composite Thin Films for Photonic Applications: Structural and Optical Properties. *ACS Omega* **2020**, *5*, 9224−9232.
(45) Zvyagina, A. I.; Aleksandrov, A. E.; Martynov, A. G.; Tameev, A. R.; Baranchikov, A. E.; Ezhov, A. A.; Gorbunova, Y. G.; Kalinina, M. A. Ion-Driven Self-Assembly of Lanthanide Bis-Phthalocyaninates into Conductive Quasi-MOF Nanowires: An Approach toward Easily Recyclable Organic Electronics. *Inorg. Chem.* **2021**, *60*, 15509−15518.
(46) Daly, S. R.; Bellott, B. J.; McAlister, D. R.; Horwitz, E. P.; Girolami, G. S. $Pr(H_3BNMe_2BH_3)_3$ and $Pr(Thd)_3$ as Volatile Carriers for Actinium-225. Deposition of Actinium-Doped Praseodymium

https://doi.org/10.1021/acsomega.1c07300
ACS Omega 2022, 7, 24973−24981

Boride Thin Films for Potential Use in Brachytherapy. *Inorg. Chem.* **2022**, *61*, 7217−7221.
(47) Karymov, M. A.; Kruchinin, A. A.; Tarantov, Y. A.; Balova, I. A.; Remisova, L. A.; Sukhodolov, N. G.; Yanklovich, A. I.; Yorkin, A. M. Langmuir-Blodgett Film Based Membrane for DNA-Probe Biosensor. *Sens. Actuators, B* **1992**, *6*, 208−210.
(48) Gorbunov, A.; Bardin, A.; Ilyushonok, S.; Kovach, J.; Petrenko, A.; Sukhodolov, N.; Krasnov, K.; Krasnov, N.; Zorin, I.; Obornev, A.; Babakov, V.; Radilov, A.; Podolskaya, E. Multiwell Photocatalytic Microreactor Device Integrating Drug Biotransformation Modeling and Sample Preparation on a MALDI Target. *Microchem. J.* **2022**, *178*, No. 107362.
(49) Gladchuk, A. S.; Krasnov, K. A.; Keltsieva, O. A.; Kalninia, Y. K.; Alexandrova, M. L.; Ivanov, N. S.; Muradymov, M. Z.; Krasnov, N. V.; Reynyuk, V. L.; Sukhodolov, N. G.; Podolskaya, E. P. A New Approach for Analysis of Polyprenols by a Combination of Thin-film Chemical Deposition and Matrix-assisted Laser Desorption/Ionization Time-of-flight Mass Spectrometry. *Rapid Commun. Mass Spectrom.* **2021**, *35*, No. e9185.
(50) Santos, J. C. C.; Pramudya, Y.; Krstić, M.; Chen, D.-H.; Neumeier, B. L.; Feldmann, C.; Wenzel, W.; Redel, E. Halogenated Terephthalic Acid "Antenna Effects" in Lanthanide-SURMOF Thin Films. *ACS Appl. Mater. Interfaces* **2020**, *12*, 52166−52174.
(51) Zheng, B.; Fan, J.; Chen, B.; Qin, X.; Wang, J.; Wang, F.; Deng, R.; Liu, X. Rare-Earth Doping in Nanostructured Inorganic Materials. *Chem. Rev.* **2022**, *122*, 5519−5603.
(52) Rappel, C.; Schaumlöffel, D. Absolute Peptide Quantification by Lutetium Labeling and NanoHPLC−ICPMS with Isotope Dilution Analysis. *Anal. Chem.* **2009**, *81*, 385−393.
(53) Zhang, K. Y.; Yu, Q.; Wei, H.; Liu, S.; Zhao, Q.; Huang, W. Long-Lived Emissive Probes for Time-Resolved Photoluminescence Bioimaging and Biosensing. *Chem. Rev.* **2018**, *118*, 1770−1839.
(54) Cheng, Y.; Shen, Z.; Zhang, Q.; Li, R.; Wei, S.; Wang, K. Lanthanides' Enhancing Absorption of Insulin and Reduction of Blood Glucose of Rat by Pulmonary Administration. *Chin. Sci. Bull.* **2000**, *45*, 604−608.
(55) Shen, Z.-C.; Cheng, Y.; Zhang, Q.; Wei, S.-L.; Li, R.-C.; Wang, K. Lanthanides Enhance Pulmonary Absorption of Insulin. *Biol. Trace Elem. Res.* **2000**, *75*, 215−225.
(56) Cheng, Y.; Li, R.; Wang, K. Changes of Conformation and Aggregation State Induced by Binding of Lanthanide Ions to Insulin. *Sci. China, Ser. B: Chem.* **2002**, *45*, 349−357.
(57) Yanklovich, M. A.; Ivanov, N. S.; Sukhodolov, N. G.; Zhukov, A. N. A Study of the Properties and Composition of Stearic Acid Monolayers on an Aqueous Subphase Containing Cadmium Ions. *Colloid J.* **2016**, *78*, 277−280.
(58) Ivanov, N. S.; Shvets, A. A.; Yanklovich, A. I.; Kondrat'ev, Y. V.; Sukhodolov, N. G. Heats of Reactions of Stearic Acid Monolayers with 3d-Metal Salts. *Russ. J. Gen. Chem.* **2016**, *86*, 1193−1194.
(59) Sauerbrey, G. Verwendung von Schwingquarzen Zur Wägung Dünner Schichten Und Zur Mikrowägung. *Zeitschrift für Phys.* **1959**, *155*, 206−222.
(60) Arslanov, V. V.; Gorbunova, Y. G.; Selektor, S. L.; Sheinina, L. S.; Tselykh, O. G.; Enakieva, Y. Y.; Tsivadze, A. Y. Monolayers and Langmuir-Blodgett Films of Crown-Substituted Phthalocyanines. *Russ. Chem. Bull.* **2004**, *53*, 2532−2541.
(61) Rabinovitch, W.; Robertson, R. F.; Mason, S. G. Relaxation of Surface Pressure and Collapse of Unimolecular Films of Stearic Acid. *Can. J. Chem.* **1960**, *38*, 1881−1890.
(62) Gershfeld, N. L. Thermodynamics and Experimental Methods for Equilibrium Studies with Lipid Monolayers. In *Methods in Membrane Biology*; Springer US: Boston, MA, 1974; pp 69−104.
(63) Heikkila, R. E.; Kwong, C. N.; Cornwell, D. G. Stability of Fatty Acid Monolayers and the Relationship between Equilibrium Spreading Pressure, Phase Transformations, and Polymorphic Crystal Forms. *J. Lipid Res.* **1970**, *11*, 190−194.

https://doi.org/10.1021/acsomega.1c07300
ACS Omega 2022, 7, 24973−24981